

“Green”, innovative, versatile and efficient carbon materials from polyphenolic plant extracts

Supplementary Material

Alain Celzard¹ and Vanessa Fierro²

Institut Jean Lamour, UMR CNRS – Université de Lorraine n°7198. ENSTIB, 27 rue Philippe Séguin, BP 21042, 88051 Epinal cedex 9, France

¹Corresponding author. Tel: + 33 372 74 96 14. Fax: + 33 372 74 96 38. E-mail address : Alain.Celzard@univ-lorraine.fr (A. Celzard)

²Corresponding author. Tel: + 33 372 74 96 77. Fax: + 33 372 74 96 38. E-mail address : Vanessa.Fierro@univ-lorraine.fr (V. Fierro)

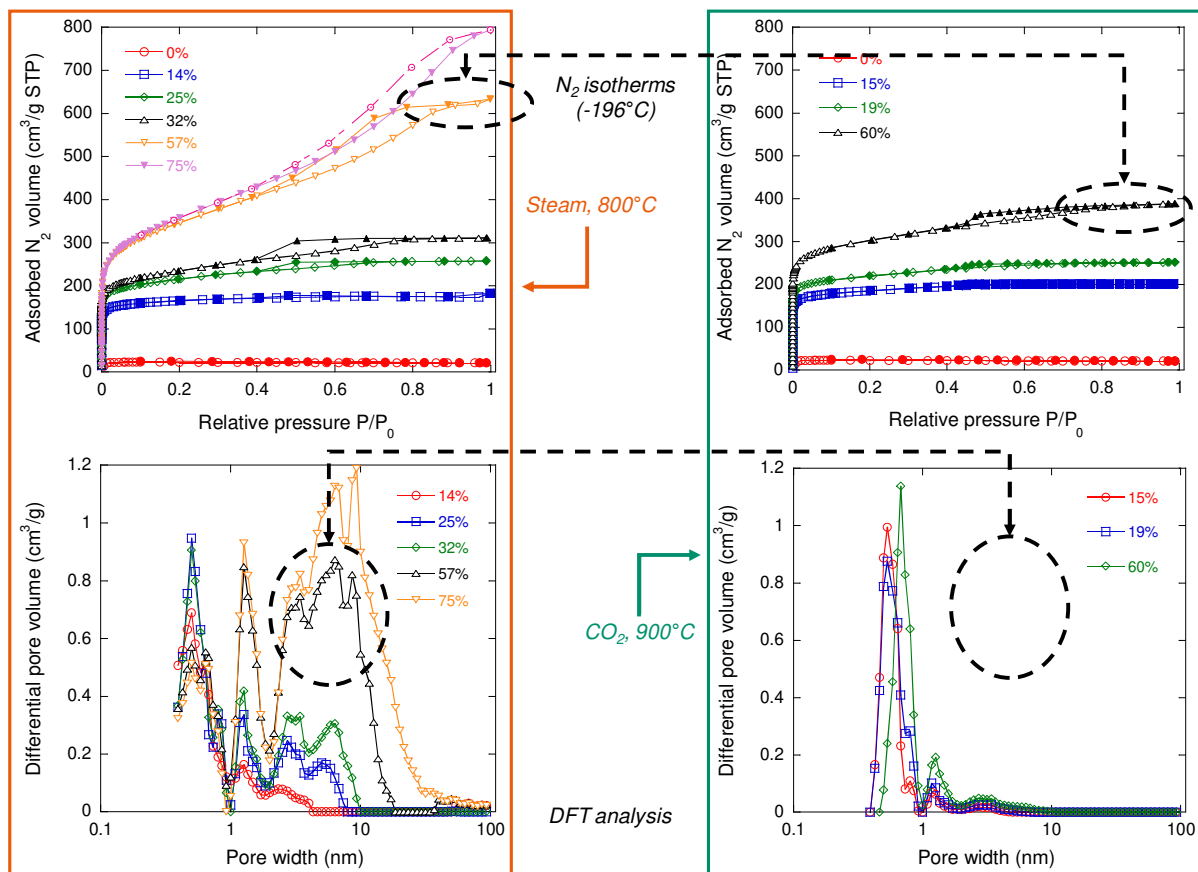


Figure S1. Effect of steam and CO₂ activation of tannin-based carbon at 800°C and 900°C, respectively, on nitrogen adsorption isotherms (top) and corresponding pore-size distributions obtained by application of the NLDFT method (bottom).

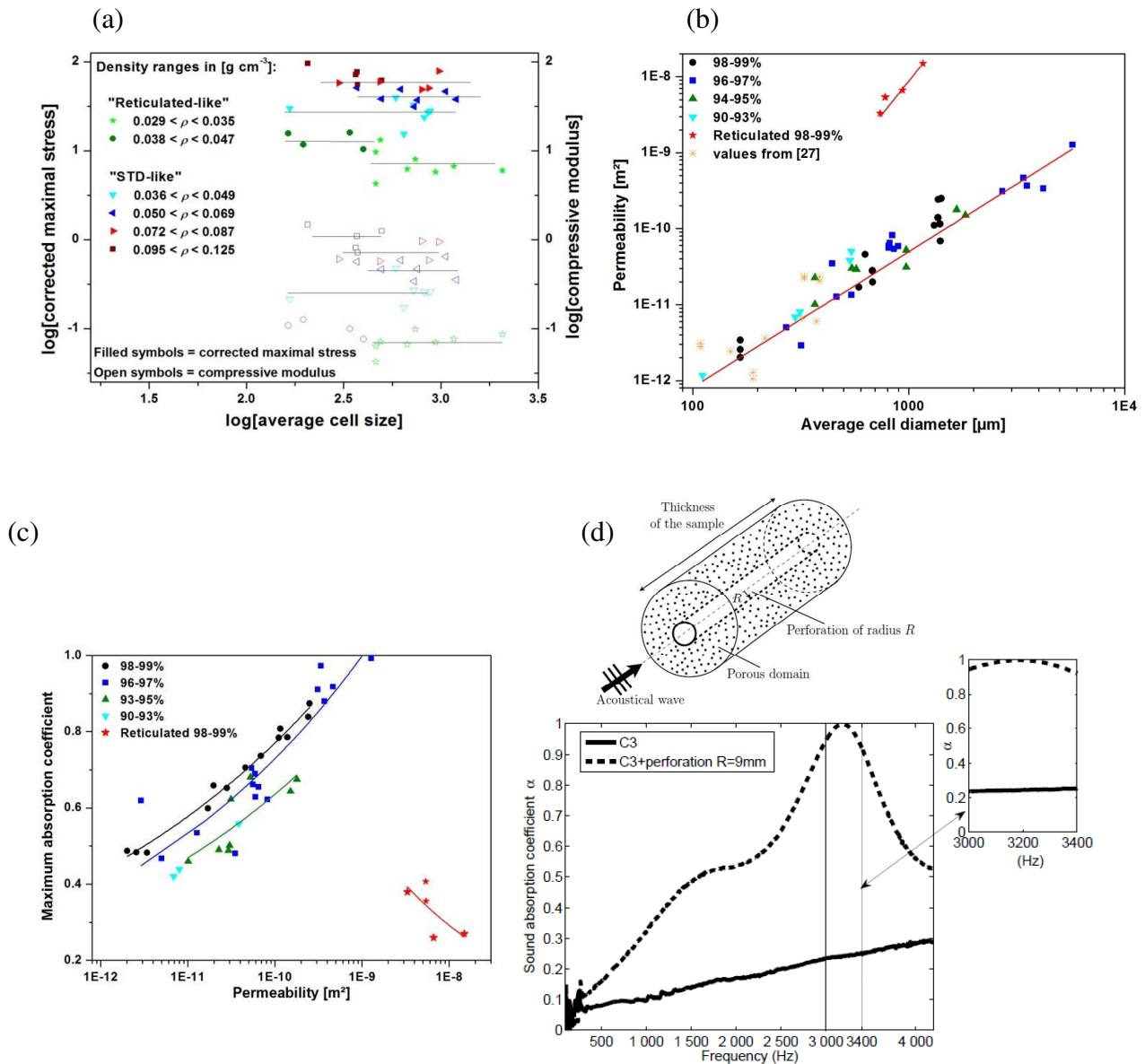


Figure S2. Physical properties of model carbon foams: (a) mechanical properties in compression; Acoustic properties through: (b) air permeability, (c) sound absorption coefficient, and (d) application of the double-positivity concept. (Reprinted from [82–84] with permission from Elsevier).

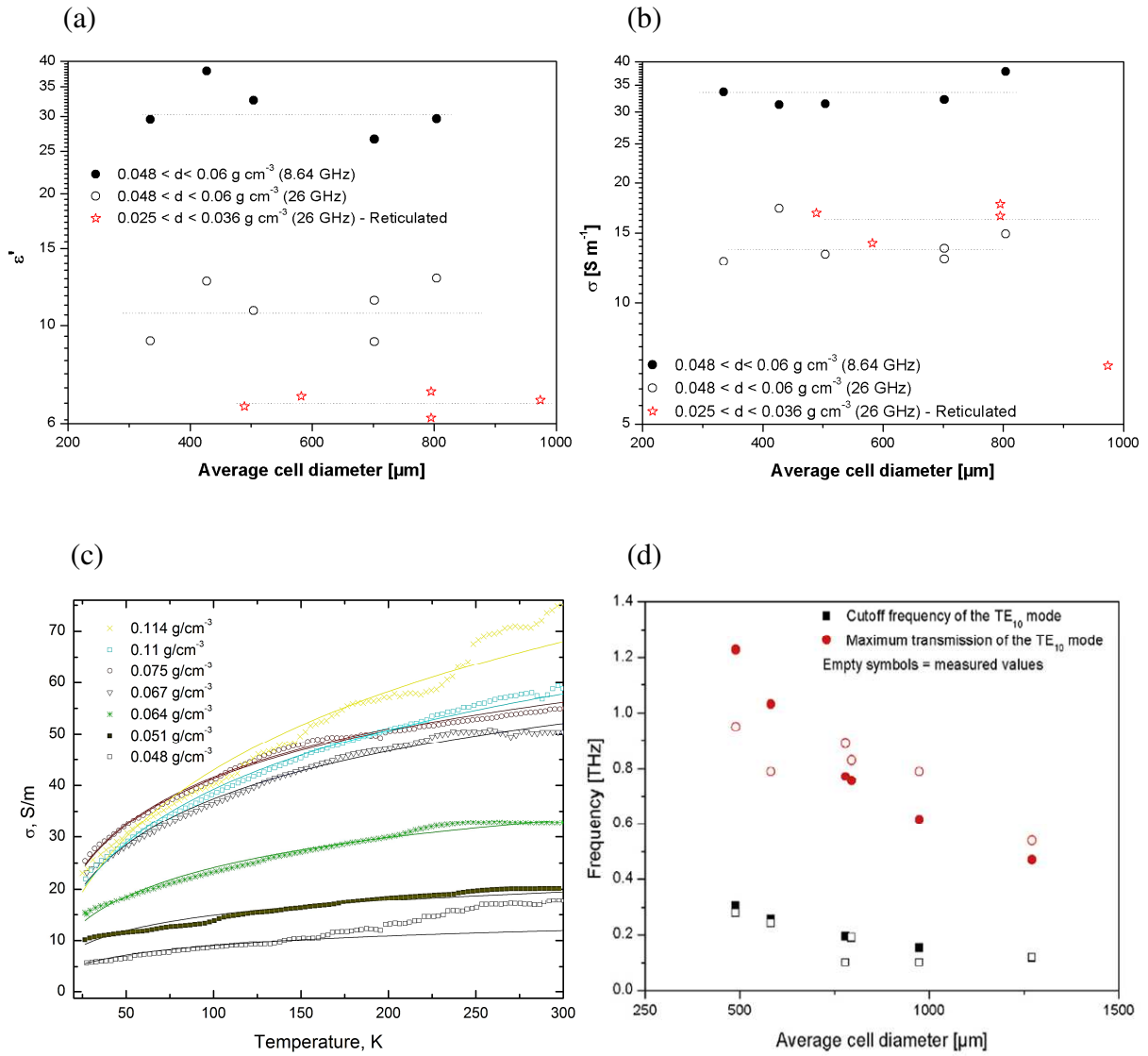


Figure S3. Physical properties of model carbon foams (continued): Electromagnetic (EM) properties in terms of (a) real part of permittivity and (b) electrical conductivity as a function of bulk density and cell size; (c) conductivity mechanism; (d) evidence of a waveguide effect in reticulated vitreous carbon foams. (Adapted and reprinted from [87] with permission from Elsevier, and from [88] with permission from IEEE).

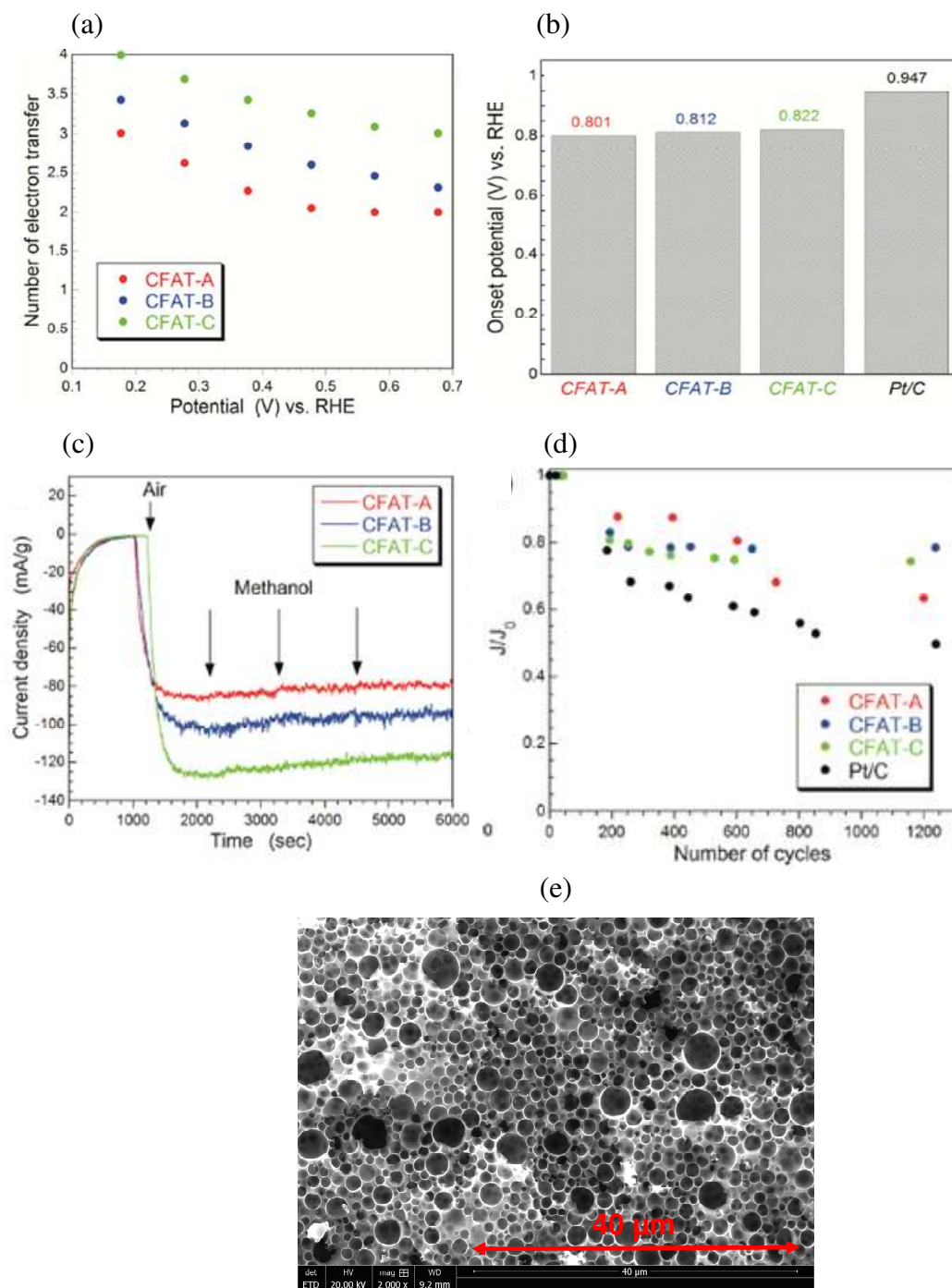


Figure S4. Electrochemical properties of tannin-based, emulsion-templated cellular carbons when used as electrocatalyst for ORR in alkaline conditions: (a) number of electron transfer; (b) onset potential; (c) changes of current density as a function of time during methanol addition; (d) normalised kinetic current density as a function of number of cycles); (e) SEM picture of the sample CFAT-C. (Adapted from [95] with permission from the American Chemical Society).

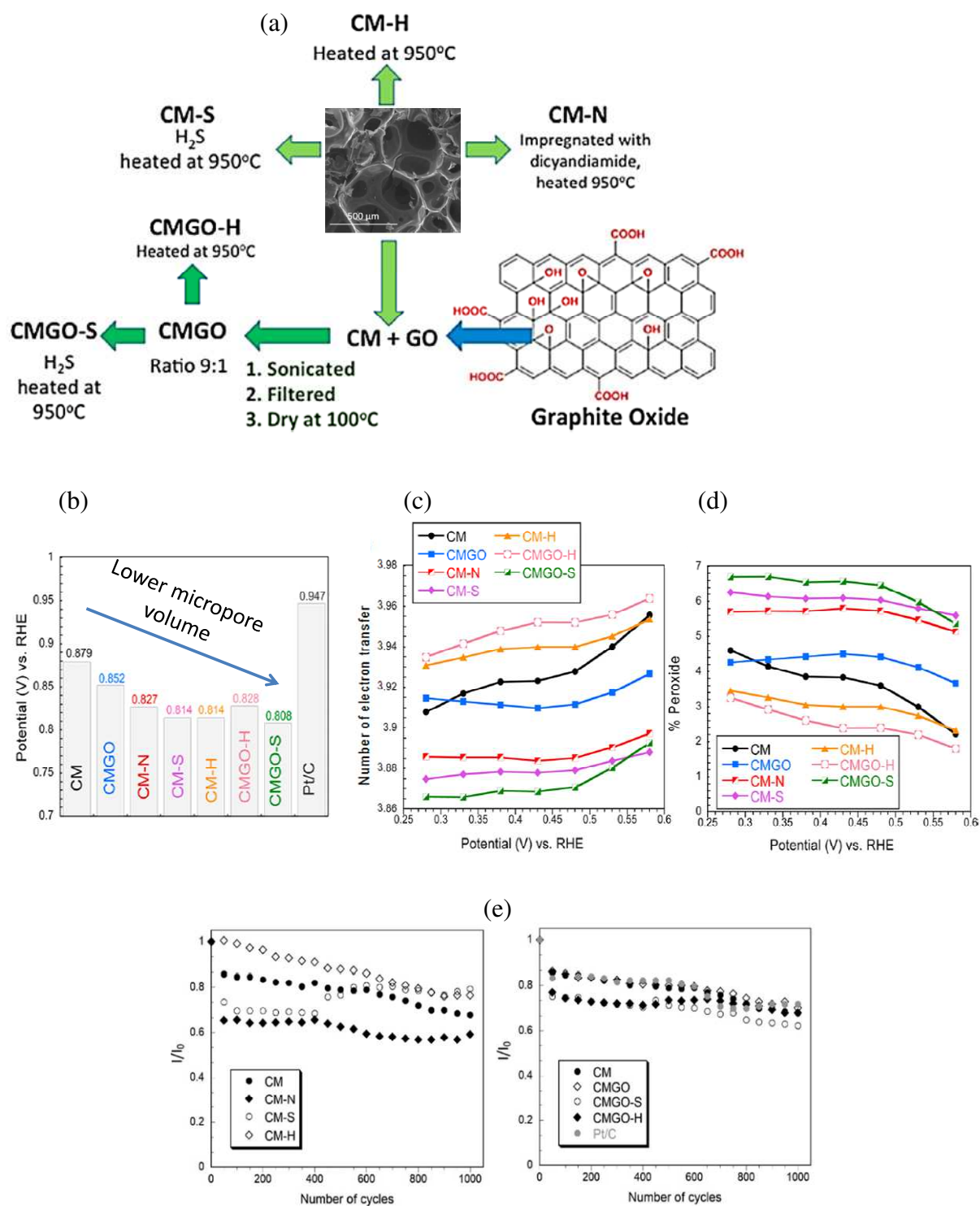


Figure S5. Electrochemical properties of tannin-based cellular carbons, as such or modified (a), derived from liquid foams obtained by whipping aqueous solutions when used as electrocatalyst for ORR: (b) onset potential; (c) number of electron transfer; (d) fraction of oxygen peroxide produced; (e) normalised kinetic current density as a function of number of cycles). (Adapted from from [97] with permission from the American Chemical Society).

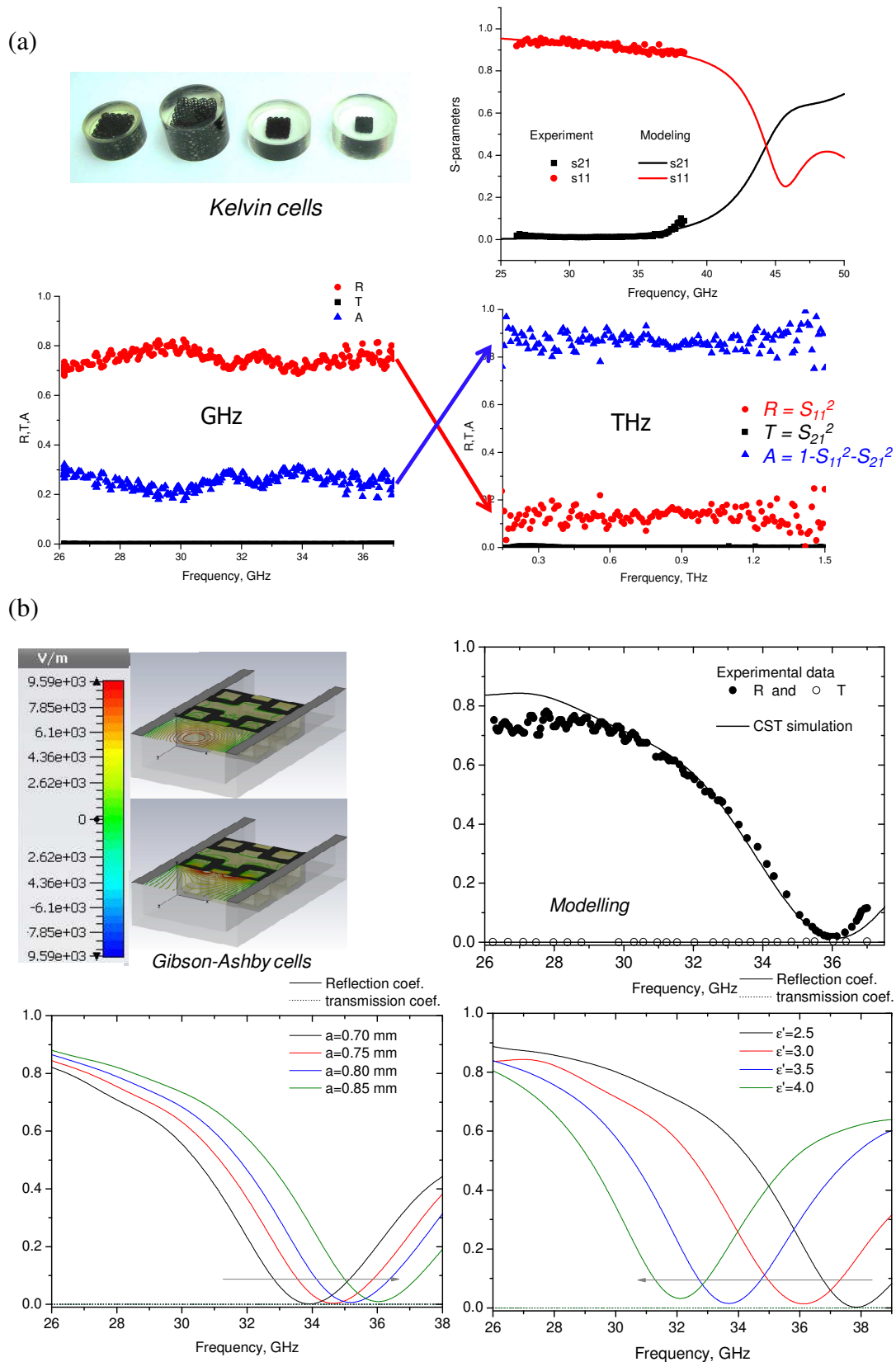
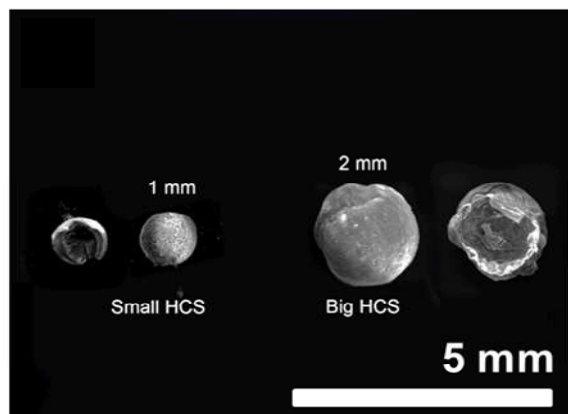
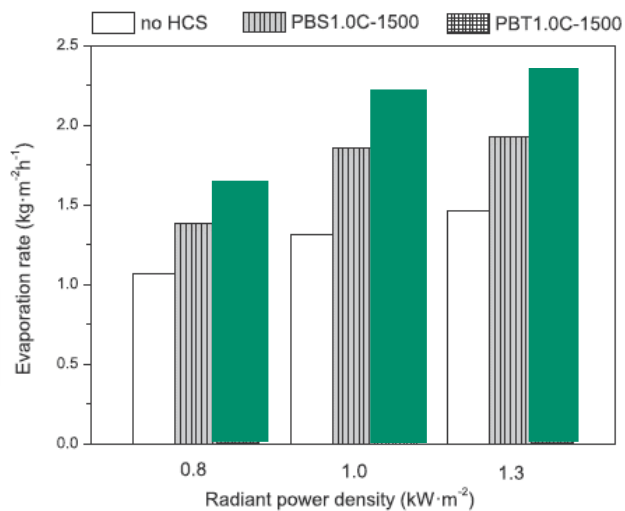


Figure S6. Electromagnetic properties in the GHz-THz range of tannin-based periodic carbon structures based on (a) Kelvin cells and (b) Gibson-Ashby cells (see text for details). (Reprinted from [98] with permission from Elsevier and from [99]).

(a)



(b)

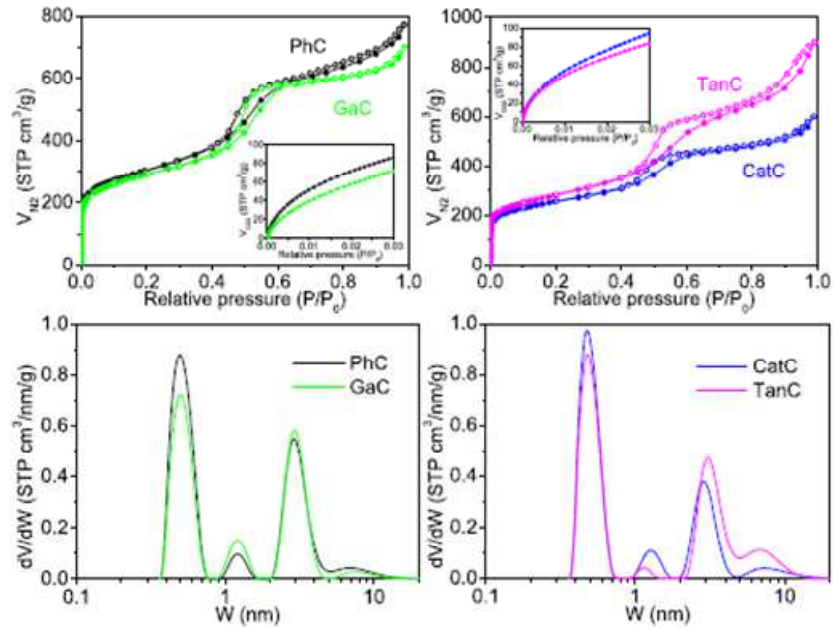


(c)



Figure S7. (a) Two sizes of hollow carbon spheres tested as floating bodies for solar evaporation (again chosen broken to reveal their empty character); (b) Evaporation rate of water under simulated solar light without (white bars) and with floating hollow carbon spheres (those based on tannin are coloured in green, no graphitisation catalyst having been used); (c) Strong magnetic character of these spheres when prepared in the presence of iron. (Adapted from [102] with permission from Elsevier).

(a)



(b)

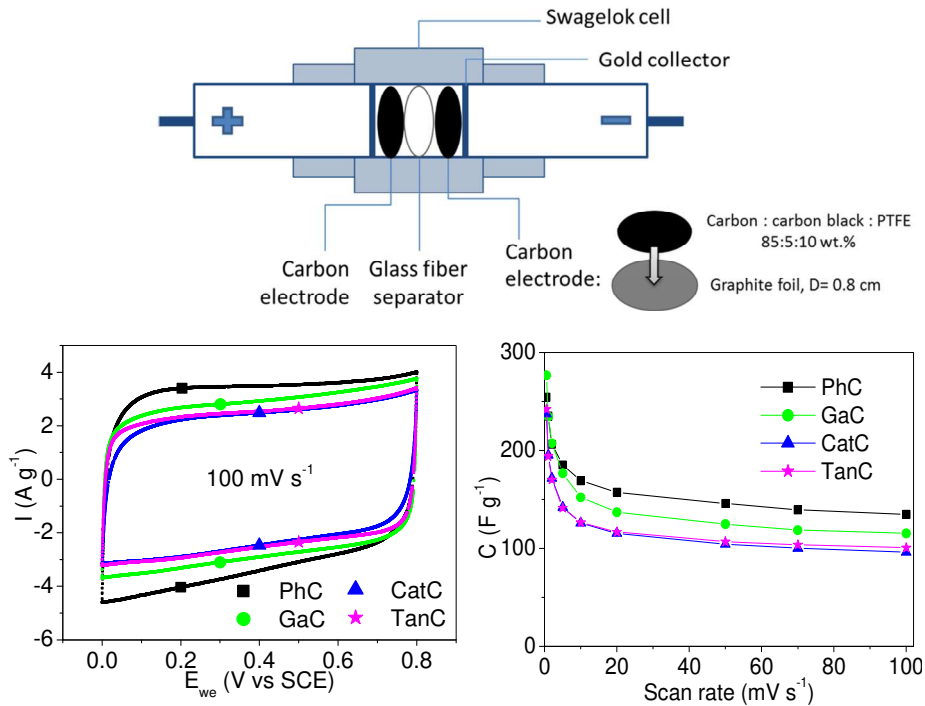


Figure S8. Ordered mesoporous carbons (OMCs) by nano-casting using SBA-15 mesoporous silica as template: (a) N_2 and CO_2 (insets) adsorption isotherms (top) and corresponding pore-size distributions (bottom); and (b) electrochemical properties in terms of cyclic voltammetry curves at a sweep rate of 100 mV/s (bottom left) and change of specific capacitance with scan rate (bottom right) when measured with a 2-electrode cell system (top). (Reprinted from [108] with permission from Elsevier).

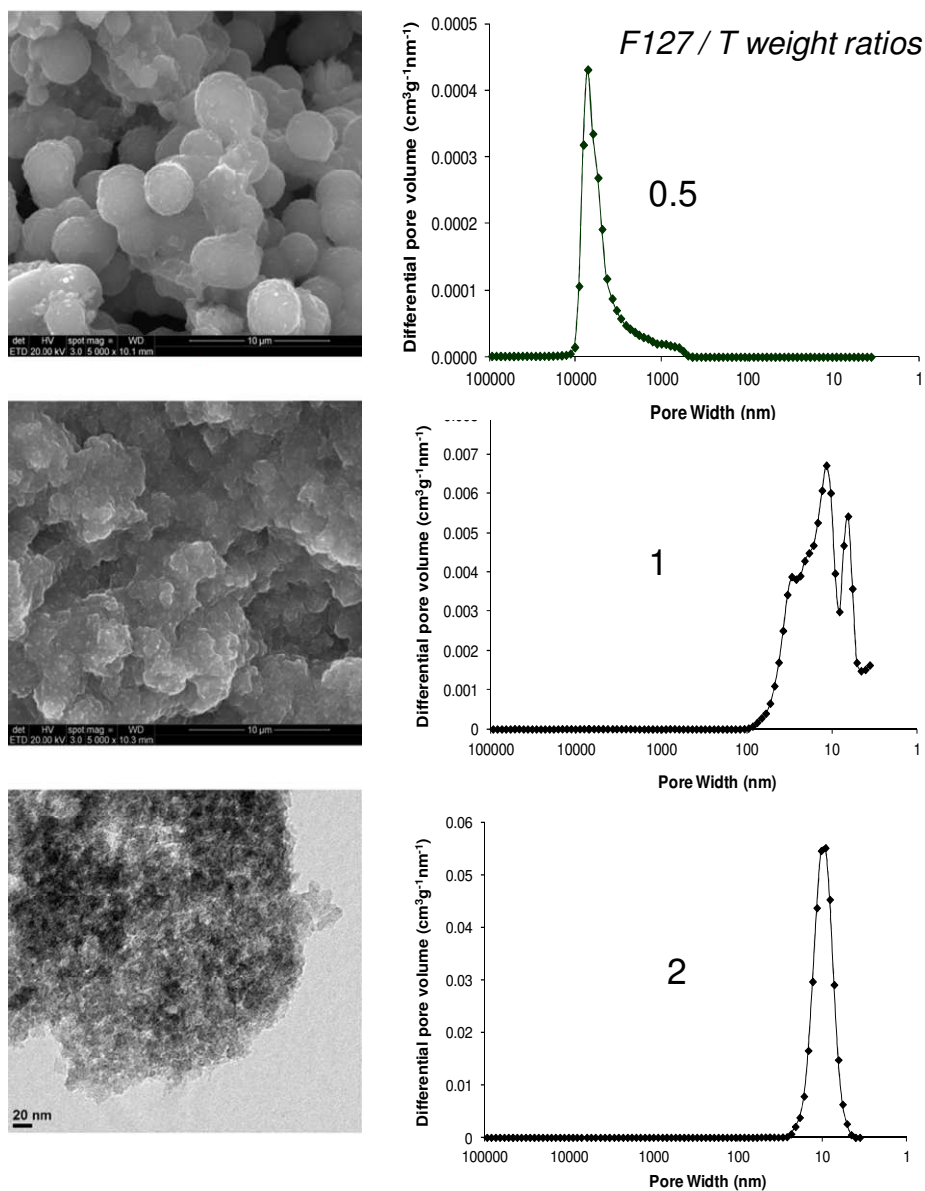


Figure S9. (b) Pore-size distributions (from Hg porosimetry only) of tannin-based carbon xerogels prepared at pH 6 and with weight ratios of triblock copolymer (F127) to tannin of 0.5, 1 and 2.

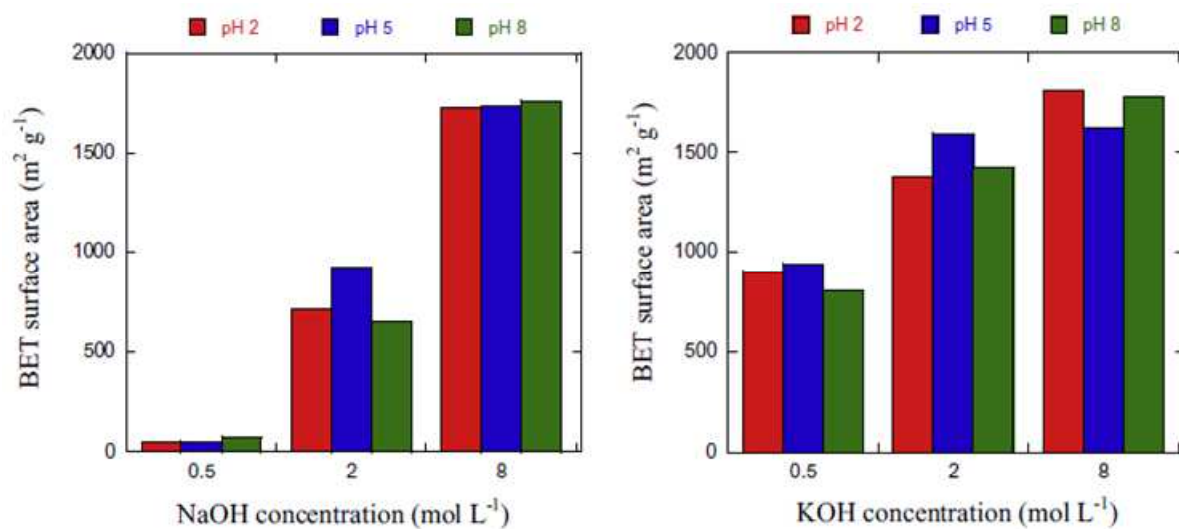


Figure S10. BET surface areas of tannin-based, activated carbon xerogels obtained by impregnation of hydrogels prepared at different pH with aqueous solutions of NaOH or KOH, followed by drying and pyrolysis at 750°C. (reprinted [128] with permission from Elsevier).

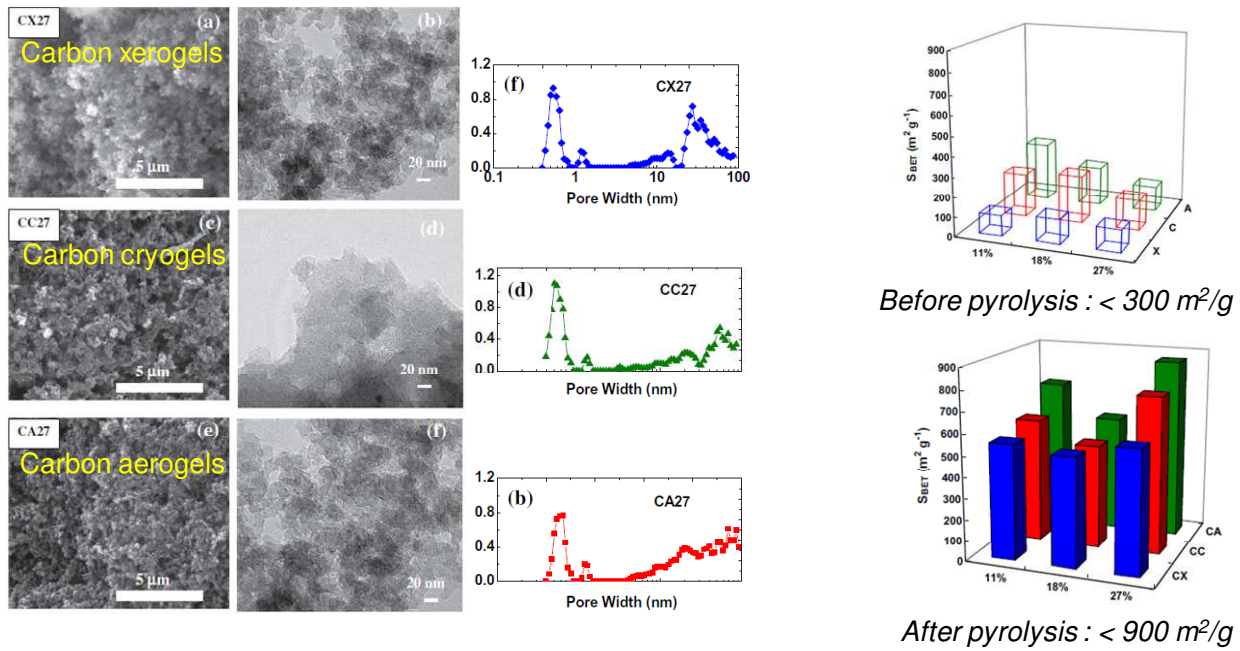


Figure S11. Materials obtained after drying and pyrolysis at 900°C of the N-doped tannin-based carbonaceous hydrogels presented in Fig. 16(b): TEM pictures (left), pore-size distributions (middle) and BET areas (right). (Adapted from [132] with permission from Elsevier).